(Received 4 January 2025, Accepted 18 February 2025, Scheduled 23 February 2025)

Novel Compact Wideband Bandpass Filters with High Upper Stopband Rejection Featuring a Quadruple-Mode Resonator

Chuan Shao[1, 2, *], Rong Cai[1, 2], Xinnai Zhang[1, 2], and Kai Xu[3]

[1] *School of Information Engineering, Jiangsu College of Engineering and Technology, Nantong 226000, Jiangsu, P. R. China*
[2] *Nantong Key Laboratory of Artificial Intelligence New Quality Technology Jiangsu College of Engineering and Technology, Nantong 226000, Jiangsu, P. R. China*
[3] *Nantong Key Laboratory of Advanced Microwave Technology, Nantong University, Nantong 226019, Jiangsu, China*

ABSTRACT: In this letter, a novel, compact bandpass filter architecture that leverages a quadruple-mode stepped impedance resonator (SIR) is introduced. This design is predicated on the principles of odd-even-mode analysis, which has been meticulously applied twice to elucidate the resonator's operational dynamics. The distinct boundary conditions inherent to the odd-odd and even-odd degenerate modes result in their splitting, a phenomenon that is pivotal to the filter's performance characteristics. The equivalent circuits representing the quadruple modes function as quarter-wavelength SIRs, a design choice that inherently confers a compact form factor upon the resonator. This is achieved without compromising the filter's functionality, as each mode contributes to the overall filtering response in a manner that is both efficient and space-saving. Furthermore, the filter is characterized by a 20-dB stopband rejection that extends up to 6.9 GHz, which corresponds to 3.8 times of the fundamental frequency (f_0). This outstanding stopband performance is a testament to the design's effectiveness in attenuating unwanted signals while maintaining a compact footprint.

1. INTRODUCTION

In the quest to meet the stringent demands of contemporary wireless communication systems, there is an acute necessity for microwave filters that exhibit high performance and compactness [1–5]. Recently, quadruple-mode resonator has emerged as a promising candidate for the design of bandpass filters [6–14], as it can gather these four modes together to construct a wideband bandpass filter [6–10] or control each mode of these four modes independently to design a dual-band or a quad-band bandpass filter [11–14].

In the realm of quadruple-mode filters, several studies have demonstrated good selectivity in the passband. For instance, in [6, 7], two quadruple-mode filters with several transmission zeros in proximity to the passband are reported, by which the selectivity has been enhanced. Additionally, bandpass filters based on a quadruple-mode resonator which cover an ultra-wideband passband from 3.1 to 10.6 GHz are studied in [8, 9]. However, the filters developed in these studies may be encumbered by their bulky sizes.

Despite the commendable performance of the aforementioned quadruple-mode filters within their respective passbands, the concurrent attainment of a compact form factor and superior stopband performance remains a formidable challenge in the domain of microwave filter design. The dual objectives necessitate a delicate balance between miniaturization and the maintenance of stringent filtering criteria, particularly in the context of modern communication systems where space is at a premium, and signal integrity is paramount [16–18].

In this letter, an innovative compact bandpass filter employing a quadruple-mode stepped impedance resonator architecture is introduced. A synergistic combination of a compact footprint and superior stopband performance is demonstrated by this design, which distinguishes it from its predecessors. To substantiate the theoretical underpinnings of our design, a prototype of the quadruple-mode filter has been fabricated and subjected to rigorous testing. The implementation of this filter serves as a tangible validation of the proposed design principles, offering empirical evidence of the filter's capabilities in achieving the desired performance metrics.

2. ANALYSIS OF THE QUADRUPLE-MODE RESONATOR

The structural configuration of the proposed quadruple-mode resonator, along with its equivalent circuit models and the associated boundary conditions, is meticulously detailed in Fig. 1. In Fig. 1, the dashed line can be regarded as a symmetry plane when the even- and odd-mode analysis is conducted. The design is based on the principles of odd-even-mode analysis, which has been carefully applied twice to explain the resonator's operational dynamics. For the purposes of explication, these four fundamental resonant frequencies of the quadruple-mode resonator are correspondingly named as f_{oo}^I, f_{eo}^I, f_{oe}^I, f_{ee}^I according to different boundary conditions. Each equivalent circuit of the quadruple-mode resonator can be basically treated as a quarter-wavelength ($\lambda_g/4$) stepped impedance resonator (SIR). When boundary conditions in Fig. 1 are neglected, the input impedance (Z_{in}) of each equivalent circuit depicted in

* Corresponding author: Chuan Shao (ch_shao@jcet.edu.cn).

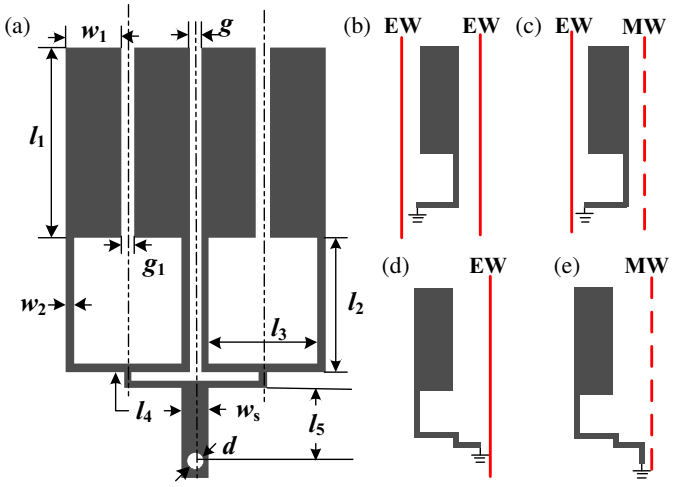

FIGURE 1. Structure of the proposed quadruple-mode SIR and its equivalent circuits. (Electric wall (EW), Magnetic Wall (MW)). (a) Structure of the proposed resonator. (b) Odd-odd mode equivalent circuit. (c) Even-odd mode equivalent circuit. (d) Odd-even mode equivalent circuit. (e) Even-even mode equivalent circuit.

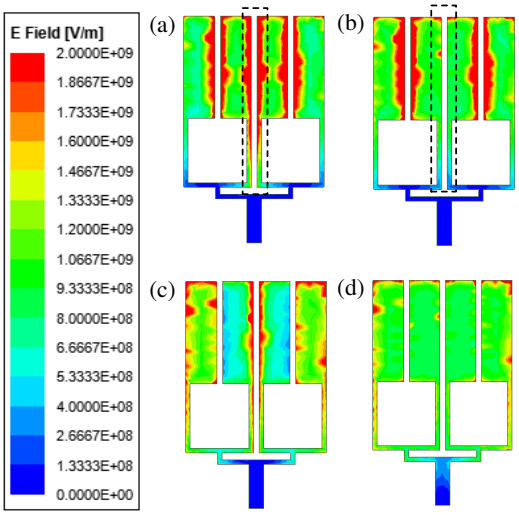

FIGURE 2. Electric field distribution of each resonant mode of the developed resonator. (a) Odd-odd mode. (b) Even-odd mode. (c) Odd-even mode. (d) Even-even mode.

Fig. 1 can be derived using established theoretical frameworks in [15].

$$Z_{in} = jZ_l \frac{Z_h \tan\theta_h + Z_l \tan\theta_l}{Z_l - Z_h \tan\theta_h \tan\theta_l} = jZ_l \frac{\tan\theta_h + R_z \tan\theta_l}{R_z - \tan\theta_h \tan\theta_l} \quad (1)$$

where Z_h and Z_l are the high-low impedances; θ_h and θ_l are the high-low electrical lengths (assuming high impedance section with same width), respectively; and $R_z = Z_l/Z_h$ is the impedance ratio. As discussed in [15], when $Y_{in} = 1/Z_{in} = 0$, the resonance condition can be obtained, and the following relationship can be given

$$R_z = \tan\theta_h \tan\theta_l \quad (2)$$

Upon setting θ_h equal to θ_l, the subsequent relationship between the fundamental (f^I) and the first harmonic frequencies (f^{II}) of the $\lambda_g/4$ SIR is obtained:

$$\frac{f^{II}}{f^I} = \frac{\pi}{\arctan\left(\sqrt{R_z}\right)} - 1 \quad (3)$$

Consequently, once the impedance ratio is established, the stopband rejection level of the proposed bandpass filter can be determined.

According to the equivalent circuits of the proposed resonator in Fig. 1 and Eq. (1), the relationship among the four fundamental resonant frequencies of the quadruple-mode resonator can be derived as follows: $f^I_{ee} < f^I_{oe} < f^I_{eo} = f^I_{oo}$ when boundary conditions are neglected. Despite the apparent structural equivalence of the odd-odd mode and even-odd mode circuits as depicted in Figs. 1(b) and 1(c), these configurations are subject to distinct boundary conditions. Specifically, the odd-odd mode is characterized by the presence of two electric walls (EWs), whereas the even-odd mode is defined by the presence of one electric wall (EW) and one magnetic wall (MW). In order to elucidate these four resonant modes and their corresponding boundary conditions with greater clarity, electric field distributions of each resonant mode of the developed resonator are depicted in Fig. 2. Referring to Fig. 2, the electric field distributions for the odd-odd mode and even-odd mode are found to be nearly identical, with the exception of the region enclosed by the dashed line. Ultimately, this discrepancy between Figs. 2(a) and 2(b) is attributed to the distinct boundary conditions. Consequently, the two degenerate modes become distinguishable when the impact of boundary conditions is significant and cannot be overlooked. As depicted in Fig. 3, there is a divergence in the modes as the parameter g diminishes, leading to a sequential ordering of the resonant frequencies such that $f^I_{ee} < f^I_{oe} < f^I_{eo} < f^I_{oo}$. Fig. 4 illustrates the frequency response of the quadruple-mode resonator with respect to l_5 under conditions of weak coupling. It is evident from Fig. 3 that f^I_{ee} can be adjusted independently, while the other resonant frequencies remain constant, demonstrating the

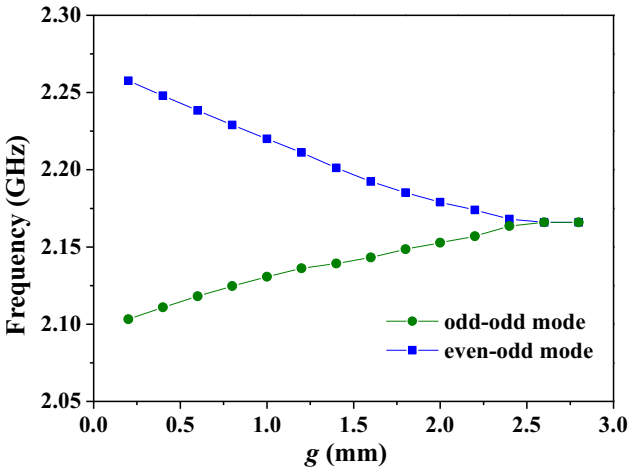

FIGURE 3. Extracted resonant frequencies of odd-odd and even-odd modes under different gap g. (Dimensions of the resonator are $w_1 = 2.1$, $w_2 = 0.3$, $w_s = 1$, $l_1 = 7$, $l_2 = 4.7$, $l_3 = 4$, $l_4 = 4$, $l_5 = 2.6$, $d = 0.6$, $g = 0.4$, $g_1 = 0.4$, unit: mm).

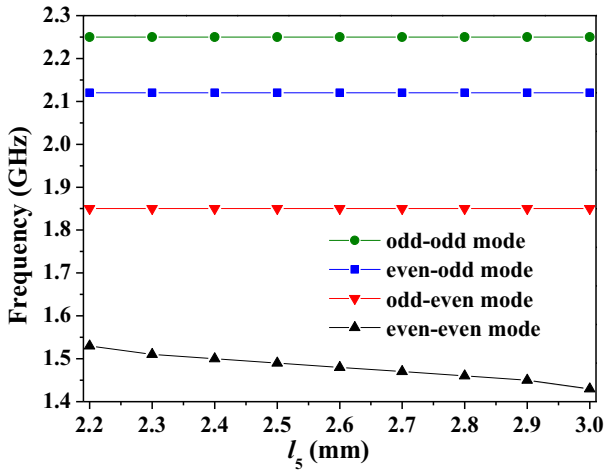

FIGURE 4. Extracted resonant frequencies of these quad modes under different length l_5. ($l_4 = 2.8$ mm, other dimensions are the same as those in Fig. 3).

selective tunability of the resonant modes within the quadruple-mode resonator framework.

3. WIDEBAND FILTERS DESIGN

In the filter design depicted in Fig. 4, the center frequency is set at 1.8 GHz, and the impedance ratio is selected as $R_z = 0.4$ with $Z_h = 115\,\Omega$ and $Z_l = 45\,\Omega$. Dimensions of the filter are given in Fig. 5. As a result, the subsequent relationship between f^{II} and f^{I} can be calculated as $f^{II}/f^{I} = 4.62$ using Eq. (3). Accordingly, four harmonic frequencies can be obtained as $f_{ee}^{II} = 6.93$ GHz, $f_{oe}^{II} = 8.55$ GHz, $f_{eo}^{II} = 9.8$ GHz, and $f_{oo}^{II} = 10.4$ GHz based on the results in Fig. 5 ($l_5 = 2.6$ mm). Ultimately, the harmonic suppression level of the filter is determined by the lowest frequency, f_{ee}^{II}.

The passband width of the bandpass filter can be adjusted by changing l_5 as discussed above in Fig. 4. Two microstrip lines with characteristic impedance $Z_0 = 50\,\Omega$ attaching coupled lines with width $w = 0.3$ mm are utilized to construct the I/O ports as shown in Fig. 5. The external quality of the filter can be altered by changing l_q and g_2.

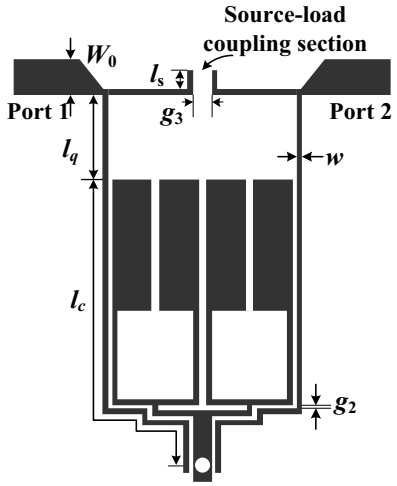

FIGURE 5. Configuration of the proposed quadruple-mode filter. (Dimensions of the filter are $W_0 = 1.9$, $w = 0.3$, $g = 0.4$, $g_2 = 0.2$, $g_3 = 1$, $l_s = 1$, $l_q = 3.5$, $l_c = 18.9$, $l_4 = 2.8$, $l_5 = 2.6$, unit: mm. Other dimensions are the same as those in Fig. 3).

In the pursuit of enhancing the selectivity of the proposed quadruple-mode filter, the incorporation of a source-load coupling (SLC) section has been strategically implemented in the design, as illustrated in Fig. 5. This design innovation is predicated on the principle that SLC can introduce additional transmission zeros, thereby improving the filter's performance without adversely affecting the passband characteristics. The simulated results of the developed filter, both with and without the SLC section, are juxtaposed in Fig. 6. Upon analysis of this figure, it is evident that the introduction of SLC has successfully generated two transmission zeros at 0.8 GHz and 3.2 GHz. These zeros arise due to the presence of two distinct signal transmission paths within the filter structure. Importantly, these transmission zeros have significantly bolstered the selectivity of the quadruple-mode filter without imparting any detrimental effects on the passband performance. Additionally, the lowest harmonic occurs at 7 GHz, which is in close agreement with the previously calculated value of 6.93 GHz.

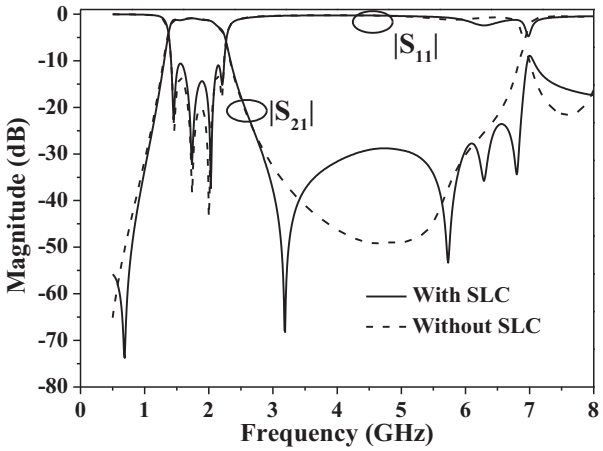

FIGURE 6. Simulated results of the proposed quadruple-mode filter without/with SLC.

4. EXPERIMENTAL RESULTS

The proposed filter has been meticulously designed and constructed on a ROGERS 4003C substrate, characterized by a dielectric constant of 3.55, a thickness of 32 mils, and a loss tangent of 0.0027, as depicted in Fig. 7. The geometric dimension of the circuit is 22×13 mm^2 ($0.22\lambda_g \times 0.13\lambda_g$). The simulation of the filter's performance was conducted using ANSYS HFSS, a high-frequency structure simulator, while the measurement of its characteristics was performed using an Agilent E5071C network analyzer, a precision instrument for evaluating the frequency response of devices. The comparison between the simulated and measured results of the quadruple-mode filter is also presented in Fig. 7. The measured passband, centered at a frequency of 1.8 GHz, exhibits a minimum insertion loss of 1 dB, which includes the losses contributed by the attached SMA connectors. The bandwidth of the filter spans 880 MHz, translat-

TABLE 1. Performance comparison with previous works.

Ref.	Insertion loss, dB	f_0, GHz	Stopband rejection level	Size, $\lambda_g \times \lambda_g$
[6]	2.7	3.65	NA	0.46×0.46
[7]	0.53	1.98	10-dB up to 5 GHz ($2f_0$)	0.22×0.2
[8]	1.1	6.85	15-dB up to 30 GHz ($4.4f_0$)	0.46×0.44
[9]	1.5	6.85	20-dB up to 27.6 GHz ($4f_0$)	0.51×0.31
[10]	NA	4.25	16.9-dB up to 17.2 GHz ($4f_0$)	0.44×0.34
This work	1.0	1.8	20-dB up to 6.9 GHz ($3.8f_0$)	0.22×0.13

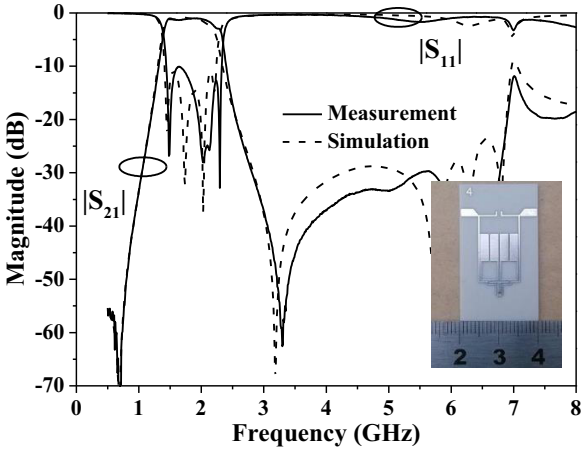

FIGURE 7. Photograph, simulated and measured results of the quadruple-mode bandpass filter with SLC.

ing to a fractional bandwidth of 49%. The filter demonstrates a stopband rejection of 20 dB, extending up to 6.9 GHz, which is equivalent to 3.8 times of the fundamental frequency (f_0). The transmission zeros, which are critical for the filter's selectivity, are observed at 0.8 GHz and 3.3 GHz.

A comprehensive comparison between the proposed filter and other quadruple-mode filters from existing literature is detailed in Table 1. It is elucidated by this table that not only is a more compact form factor exhibited by the proposed filter, but also comparable stopband performance is maintained. The smaller size and equivalent stopband performance of the proposed filter suggest a potential for improved integration into compact communication systems without compromising on performance. This advancement could be attributed to the innovative design strategies employed, which warrant further exploration and potential application in the development of next-generation microwave filters.

5. CONCLUSION

An innovative compact bandpass filter leveraging a quadruple-mode SIR is reported in this letter. This design has been meticulously analyzed through theoretical examination and substantiated by empirical validation. The stopband rejection of the filter, which extends up to 6.9 GHz, reaches 20 dB. This frequency range corresponds to 3.8 times of the fundamental frequency. In addition, the size is only $22 \times 13\,\text{mm}^2$ ($0.22\lambda_g \times 0.13\lambda_g$). When being juxtaposed with existing quadruple-mode bandpass filters, the proposed filter demonstrates good stopband performance. The congruence between simulated and measured results is exemplary, underscoring the accuracy of our design predictions and the reliability of the filter's performance.

ACKNOWLEDGEMENT

This work is supported partially by Nantong Key Laboratory of Artificial Intelligence New Quality Technology, Jiangsu College of Engineering and Technology.

REFERENCES

[1] Arif, K., K. V. P. Kumar, R. K. Barik, and G. Chakaravarthi, "A planar quad-band bandpass filter employing transmission lines loaded with tri-stepped impedance open- and dual-stepped impedance short-ended resonators," *Progress In Electromagnetics Research C*, Vol. 147, 65–72, 2024.

[2] Sun, X., C. Rong, H. Gao, and M. Zhang, "A miniaturization dual-passband microwave filter based on load-coupled open stub lines," *Progress In Electromagnetics Research Letters*, Vol. 124, 17–21, 2025.

[3] Chang, H., W. Sheng, J. Cui, and J. Lu, "Multilayer dual-band bandpass filter with multiple transmission zeros using discriminating coupling," *IEEE Microwave and Wireless Components Letters*, Vol. 30, No. 7, 645–648, 2020.

[4] Zhang, Z.-C. and W.-L. Luo, "A novel triple-mode bandpass filter using half-wavelength-resonator-coupled square-loop resonator," *Progress In Electromagnetics Research Letters*, Vol. 78, 31–37, 2018.

[5] Gao, M., Y. Yang, J. Nan, H. Wu, X. Wang, and X. Cui, "A dual transmission zero bandpass filter employing novel hairpin-coupled resonators for improved stopband characteristics application the vital signs detection radar," *Progress In Electromagnetics Research M*, Vol. 129, 11–22, 2024.

[6] Liang, C., Y. Liu, T. Liu, and F. Tai, "Bandpass filter design using quad-mode stub-loaded loop resonator," in *2019 International Applied Computational Electromagnetics Society Symposium — China (ACES)*, Vol. 1, 1–2, Nanjing, China, 2019.

[7] Görür, A. K., E. Doğan, and A. Görür, "Single-wideband and dual-band bandpass filters based on compact quadruple-mode resonator," *Journal of Electromagnetic Waves and Applications*, Vol. 38, No. 3, 327–344, 2024.

[8] Wong, S. W. and L. Zhu, "Quadruple-mode UWB bandpass filter with improved out-of-band rejection," *IEEE Microwave and Wireless Components Letters*, Vol. 19, No. 3, 152–154, 2009.

[9] Zhu, H. and Q.-X. Chu, "Ultra-wideband bandpass filter with a notch-band using stub-loaded ring resonator," *IEEE Microwave*

and Wireless Components Letters, Vol. 23, No. 7, 341–343, 2013.

[10] Deng, H.-W., Y.-J. Zhao, L. Zhang, X.-S. Zhang, and L. Qiang, "Quadruple-mode broadband BPF with sharp skirt and wide upper-stopband performance," *Microwave and Optical Technology Letters*, Vol. 53, No. 7, 1663–1666, 2011.

[11] Sun, M., Z. Chen, T. Zuo, Z. Zuo, and A. Zhang, "A high selectivity dual-band bandpass filter using quadruple-mode multi-stub loaded ring resonator (SLRR)," *International Journal of RF and Microwave Computer-Aided Engineering*, Vol. 31, No. 7, e22667, 2021.

[12] Sun, S.-J., T. Su, K. Deng, B. Wu, and C.-H. Liang, "Compact microstrip dual-band bandpass filter using a novel stub-loaded quad-mode resonator," *IEEE Microwave and Wireless Components Letters*, Vol. 23, No. 9, 465–467, 2013.

[13] Liu, H., B. Ren, X. Guan, J. Lei, and S. Li, "Compact dual-band bandpass filter using quadruple-mode square ring loaded resonator (SRLR)," *IEEE Microwave and Wireless Components Letters*, Vol. 23, No. 4, 181–183, 2013.

[14] Zhang, F., Y. Gao, Y. Wang, Y. Zhang, Y. Dong, and J. Xu, "Highly compact quad-band bandpass filter with flexibly controllable passbands," *Electronics Letters*, Vol. 57, No. 7, 276–278, 2021.

[15] Zhang, S. and L. Zhu, "Synthesis design of dual-band bandpass filters with λ/4 stepped-impedance resonators," *IEEE Transactions on Microwave Theory and Techniques*, Vol. 61, No. 5, 1812–1819, 2013.

[16] Li, C., M. Li, Z. Li, S. Cao, and R. Bai, "Dual-band filters with adjustable bandwidth and wide stopband using CRLH transmission line theory," *Progress In Electromagnetics Research C*, Vol. 152, 73–80, 2025.

[17] Tang, L., W. Han, H. Wei, and Y. Li, "Two compact hybrid band-pass filters using eighth-mode substrate-integrated waveguide and microstrip resonators," *Progress In Electromagnetics Research C*, Vol. 151, 167–175, 2025.

[18] Li, Z., C. Li, and M. Li, "Design and experimental study of dual-band left-handed filters for sub-6G applications," *Progress In Electromagnetics Research C*, Vol. 151, 45–56, 2025.